Radiocarbon, Vol 61, Nr 6, 2019, p 1823–1834 DOI:10.1017/RDC.2019.97
Selected Papers from the 23rd International Radiocarbon Conference, Trondheim, Norway, 17–22 June, 2018

EFFECT OF CRYSTALLINITY OF APATITE IN CREMATED BONE ON CARBON EXCHANGES DURING BURIAL AND RELIABILITY OF RADIOCARBON DATING

M Minami[1]* • H Mukumoto[2] • S Wakaki[3] • T Nakamura[1]

[1]Institute for Space-Earth Environmental Research, Nagoya University, Nagoya 464-8601, Japan
[2]Graduate School of Environmental Studies, Nagoya University, Nagoya 464-8601, Japan
[3]Kochi Institute for Core Sample Research, Japan Agency for Marine-Earth Science and Technology (JAMSTEC), Kochi 783-8502, Japan

ABSTRACT. This study characterized cremated bone to better understand isotope exchanges during burial, using archeological samples. The cremated bones of Jokei, a Buddhist monk (AD 1155–1213), found in an urn from the Jisho-in Temple, Nara Prefecture, Japan, were used for the analysis. ^{14}C dates were determined for eight of Jokei bone fragments of different colors (black, gray, and white). The white fragments had the highest x-ray diffractometry (XRD) crystallinity index (CI) values (0.89–1.05), Fourier-transform infrared spectroscopy (FTIR) splitting factor values (IRSF) of 5.3–7.1, and the lowest Ba concentrations. The calibrated date of the white bone fragments is 1152–1216 cal AD, consistent with Jokei's lifespan, showing these fragments yield reliable ^{14}C ages. Meanwhile, the black and gray fragments, which probably experienced lower temperatures during cremation, had lower CI and IRSF values of 0.25–0.46 and 4.2–4.9, respectively, and higher Ba concentrations. The black and gray fragments tended to show unreliable younger ^{14}C dates and higher $^{87}Sr/^{86}Sr$ values close to the soil value due to soil contamination. The results in this study indicate that it is important to check crystallinity of apatite and soil contamination using chemical indexing methods such as Ba capture, to clarify the reliability of ^{14}C dates for cremated bone samples.

KEYWORDS: bioapatite, cremated bone, crystallinity, radiocarbon.

INTRODUCTION

Bone comprises densely compacted organic molecules, including collagen fibrils, within a strongly bonded inorganic mineral structure. Collagen is a scleroprotein that contains 95% of bone carbon (Zazzo et al. 2009) and is commonly used for radiocarbon (^{14}C) dating, as it is not particularly susceptible to chemical weathering. However, it cannot be used for dating of cremated bone because it is easily destroyed by heat. Bone apatite is an inorganic mineral bone component, which is a form of calcium phosphate, $Ca_{8.3}X_{1.7}(PO_4)_{4.3}(HPO_4, CO_3)_{1.7}(OH, CO_3)_{0.3}Y_{1.7,}$ where X and Y indicate ions substituted in vacancies (Cazalbou et al. 2004)

The apatite in bone contains ~1 wt% C because carbonate (CO_3^{2-}) can be substituted for phosphate (PO_4^{3-}) or the hydroxyl (OH^-) in the crystalline structure, and this C can be used for ^{14}C dating. Furthermore, strontium (Sr) substitutes for Ca, because both these alkaline earth elements, with a valence of +2, have almost the same chemical properties, and the ionic radius (1.18 Å) of Sr^{2+} is nearly the same as that of Ca^{2+} (1.00 Å). The Sr-uptake chain system enables $^{87}Sr/^{86}Sr$ ratios to be used for many purposes such as the tracing of ancient human migration patterns (e.g. Ericson 1985; Prince et al. 2002; Hodell et al. 2004; Thornton 2011).

Bone apatite is often poorly crystallized and prone to being recrystallized and experiencing isotopic exchange with dissolved inorganic carbon derived from burial soil. Bone apatite has therefore been traditionally considered unsuitable for ^{14}C dating, due to the difficulty of removing external carbon, such as carbon from secondary carbonates (e.g. Olson and Broecker 1961; Berger et al. 1964). However, recent studies have reported that secondary carbonate contaminant in bone can be selectively removed by pretreatment with 1.0 M

*Corresponding author. Email: minami@isee.nagoya-u.ac.jp.

acetic acid for 12–24 hr (e.g. Lanting et al. 2001; Zazzo et al. 2013), or pretreatment with 0.1 M acetic acid for 1 hr (e.g. Balter et al. 2002).

Cremated bone exposed to temperatures above 600°C is reported to contain highly crystalline apatite, which is not easily affected by exogenous contaminants (Lanting et al. 2001), although atmospheric and/or fuel-wood carbon is incorporated into bone apatite structure during the cremation process (e.g. Surovell 2000; Munro et al. 2008; Snoeck et al. 2014). Japan has had a cremation culture since ancient times, and the cremation methods were spread by Buddhism from about AD 700 during the Nara period. There are many archeological samples of cremated bones that have not been dated in Japan; so being able to perform reliable ^{14}C dating of bone apatite in cremated bones would be of profound use. The aims of this study, therefore, are to establish a method to assess the reliability of dates generated by ^{14}C dating of cremated bones using apatite crystallinity and chemical indexes such as chemical and isotope compositions, and to perform reliable ^{14}C dating of cremated bone samples.

ANALYTICAL METHODS

Materials

The archaeological samples were cremated human bone fragments excavated from the Jisho-in Temple, Sango-cho, Nara Prefecture. Originally the Soji-ji Temple, the Jisho-in Temple was restored by a Buddhist monk, Gedatsu Shonin Jokei (AD 1155−1213). An urn containing cremated bone fragments was found under a stone pagoda (Jokei's tomb) located near the temple, and the remains are considered to be Jokei's alone (Mukumoto et al. 2017). The bone fragments in the urn were homogeneous, but conveniently divided into four layers (termed Layers 1−4 in this manuscript). Soil was present only in the upper parts in the urn, so samples from the upper layers were more likely to have experienced soil contamination. Eight bone fragments (> 1 cm in size) of different colors (black, gray, and white) from Layers 2–4 were analyzed. Samples Jsi-2-B2 and Jsi-4-B4 were divided into white parts (Jsi-2-B2W and Jsi-4-B4W) and black parts (Jsi-2-B2B and Jsi-4-B4B), and both were analyzed. The bone fragments were repeatedly ultrasonicated in distilled water, lyophilized, and pulverized in an agate mortar.

To investigate the influence of surrounding soil on bone during burial, chemical compositions and Sr isotope ratio of soils from within the Jokei's urn (Jsi-In) and soil (Jsi-S) around the Jisho-in Temple were compared. Bulk Sr fractions and exchangeable Sr fractions in soils were also measured because exchangeable Sr can be related to Sr in biological samples such as bones (Minami and Suzuki 2018).

Methods

Bone Treatment for ^{14}C Measurement

For extraction of bone apatite, the powdered samples were treated under vacuum with acetic acid as described by Balter et al. (2002) to remove secondary carbonate. First, about 1 g of powder was placed in a sample vial and the vial was put in a 300 mL flask containing 60 mL of 0.1 M acetic acid. After evacuating, the sample was allowed to react with the acetic acid for 1 hr. This short acid treatment accelerates removal of secondary carbonate in bones and minimizes sample loss (Balter et al. 2002). The CO_2 extracted by the acetic acid treatment was collected and purified cryogenically. Next, the sample–acid mixture was

https://doi.org/10.1017/RDC.2019.97 Published online by Cambridge University Press

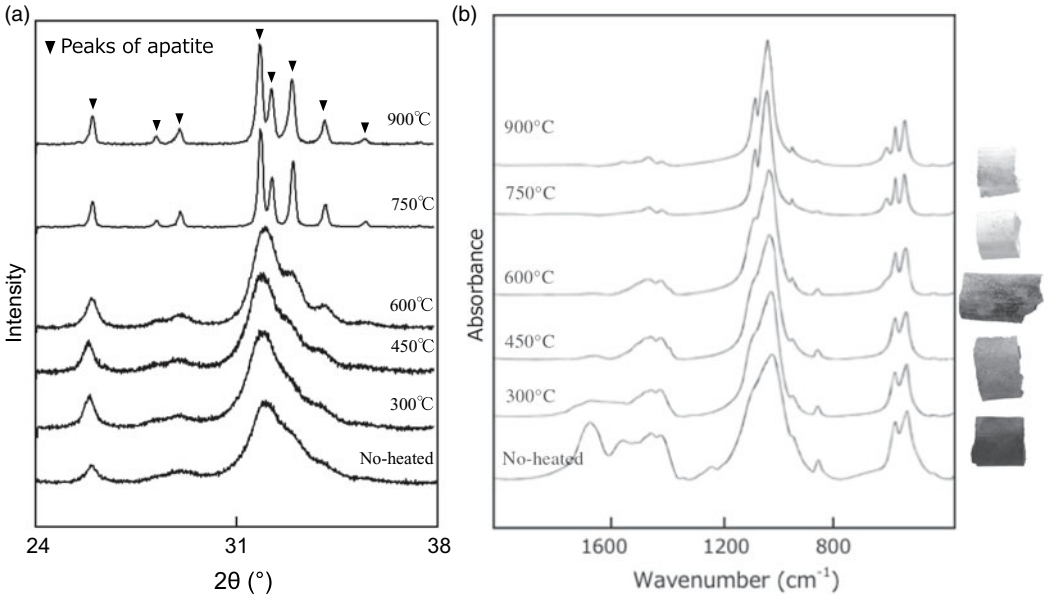

Figure 1 (a) XRD patterns and (b) IR spectra of modern boar bones heated at various temperatures together with photographs of the heated samples.

centrifuged and the residue washed repeatedly with Milli-Q water to remove all acetic acid before being lyophilized. About 200 mg of the treated bone powder was then reacted under vacuum with 85% phosphoric acid of 3 mL under vacuum for ~12 hr to extract CO_2 produced from the bone apatite.

Carbon and nitrogen contents of bone samples were determined using an elemental analyzer (Vario EL cube, Elementar). Fourier-transform infrared spectroscopy (FTIR) and x-ray diffractometry (XRD) were also performed on bone samples. FTIR analyses of bone samples (5–10 mg) was performed using a Perkin Elmer Spectrum 2000 system, by accumulating 50 scans with a spectral resolution of 4 cm^{-1} using KBr pellets, at the University of Tokyo, Japan. Powder XRD analyses of bone samples (~300 mg) involved a Rigaku MiniFlex system with CuK_α radiation. XRD patterns (Figure 1) were collected from 24° to 38° 2θ, with a 0.010° step size, and a scan speed of 0.100° min^{-1}.

An aliquot of the CO_2 gas extracted from bone apatite by the acetic acid treatment and produced from bone apatite was reduced to graphite by reaction with H_2 over an Fe catalyst at 620°C for 6 hr (Minami et al. 2013). The graphite was loaded into a sample holder and ^{14}C content was determined by accelerator mass spectrometry (AMS; Tandetron HVEE model 4130-AMS) at Nagoya University, Japan. The ^{14}C dates were calibrated using OxCal v.4.3.2 (Bronk Ramsey 2009) based on the calibration curve data of IntCal13 (Reimer et al. 2013). The other aliquots of the CO_2 gases were used to measure the carbon isotope ratio ($\delta^{13}C_{VPDB}$) by isotope ratio mass spectrometry (IRMS; Finnigan MAT-252).

Bone and Soil Treatments for Chemical and Sr Isotope Analyses

After pretreatment with acetic acid, the bone samples were heated in a muffle furnace at 825ºC for 5 hr to remove organic matter. Between 10–50 mg of each sample was dissolved in a Teflon

https://doi.org/10.1017/RDC.2019.97 Published online by Cambridge University Press

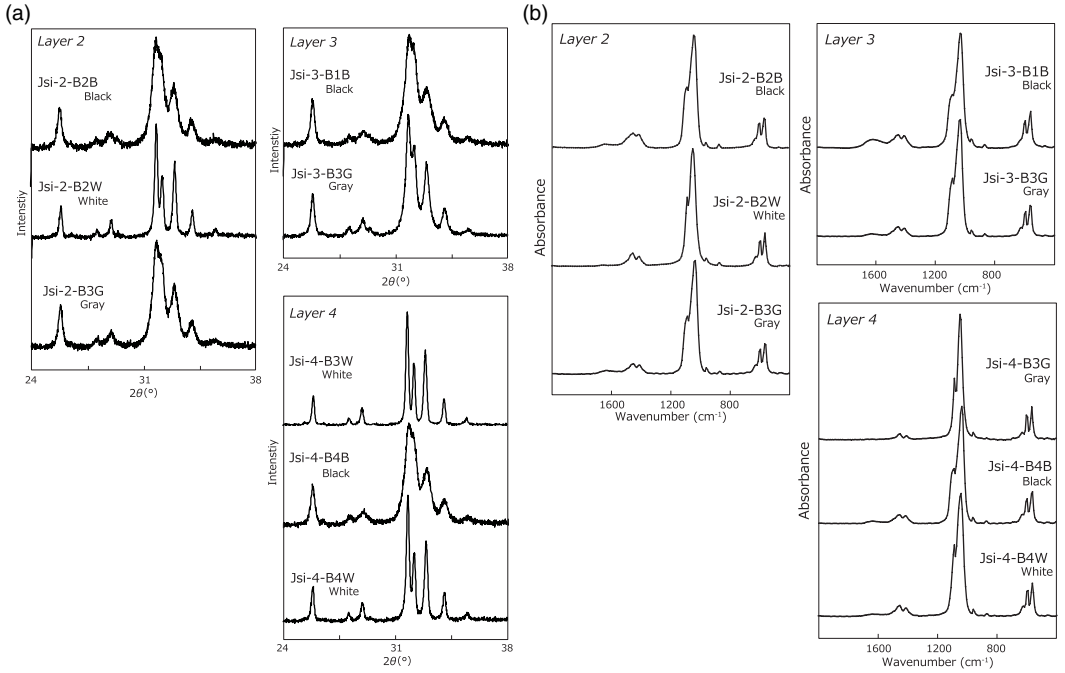

Figure 2 (a) XRD patterns of Jokei's cremated bones. (b) IR spectra of Jokei's cremated bones.

beaker for 2 hr in 2.4 M HCl, and dried on a hot plate at 120–140°C and dried, followed by digestion with concentrated HNO_3. For analysis of bulk Sr, soil samples were heated in a muffle furnace at 825°C for 3 hr to remove organic matter. Between 30–200 mg of each soil sample was digested using a mixture of 2:1 HF and $HClO_4$. For analysis of exchangeable Sr in the soils, approximately 300 mg of each sample was placed in a PE tube with 8 mL of 1 M CH_3COONH_4 and shaken for 2 hr to extract the exchangeable Sr fraction. The solution was then centrifuged at 3000 rpm for 10 min and divided into supernatant and residue. The supernatant was dried on a hot plate and digested using a few drops of concentrated HNO_3. The bulk Sr and exchangeable Sr fractions were dried and dissolved in HNO_3.

Quantitative and isotopic analyses of bones and soils were measured at the Kochi Core Center, Japan. Sr was separated from major cations by extraction chromatography using Sr spec resin (Eichrom). $^{87}Sr/^{86}Sr$ values were measured by TIMS (Thermo TRITON). The chemical composition was also measured by an inductively coupled plasma mass spectrometer (ICP-MS: Agilent7700) at the Kochi Core Center.

RESULTS

Mineralogical Changes in Bone Caused by Heating

XRD patterns of heat-treated Go-ino bones are shown in Figure 2a. The bones heated at < 600°C display a broad peak at 2θ values between 31° and 34°, with the highest intensity at ~32°. The broad peak gradually splits into three distinct crystalline peaks at 2θ values of ~32°, 32.4°, and 33° at temperatures above 600°C. The sharp patterns at 750°C and 900°C are very similar to

https://doi.org/10.1017/RDC.2019.97 Published online by Cambridge University Press

the pattern of the mineral apatite, indicating a diminished organic component and the formation of pure crystalline hydroxyapatite. Crystal index (CI) values calculated from the refraction peaks in XRD patterns provide a semi-quantitative means of estimating crystallinity changes in bone phosphate (Person et al. 1995). The CI values of heat-treated samples were 0 at < 450°C, 0–0.5 at 450°C–600°C, and > 0.9 above 750°C.

Bone IR spectra of heat-treated bones are shown in Figure 2b. The IR spectra indicate absorbance bands of carbonate at 710, 874, and 1415 cm^{-1} and phosphate at 605 and 1035 cm^{-1} (Olsen et al. 2008; Pramanik et al. 2013). IR spectra of the burnt bone samples display a decrease in the broad peak of organic matter and water between 1700 and 1600 cm^{-1} with increasing temperature. This peak is barely detectable with samples burnt above 600°C. The broad PO_4 bands around 1000 cm^{-1} and two anti-symmetric PO_4 bands at 565 and 605 cm^{-1} become sharper as temperature increases. The CO_3 absorbance peaks (1550–1400 cm^{-1} and 880 cm^{-1}) decrease with increasing temperature. IRSF values are also used as a crystallinity index, measured for the two bands of PO_4 at 565 and 605 cm^{-1}. The IRSF calculation procedure outlined by Weiner and Bar-Yosef (1990) was followed. The IRSF values increase from 3 to 7 as the temperature increases. This result is consistent with the experimental results reported in Hüls et al. (2010), which show an increase in IRSF from 3 at 500°C to > 5 at 800°C during burning under wet conditions. The IR spectra indicate that at < 600°C, organic material begins to burn (which decreases amide peaks at ~1700–1200 cm^{-1}) and eventually disappears. The disappearance is coupled with the removal of substituted CO_3 (lowering of CO_2 vibrations at ~1450, ~1415, and ~870 cm^{-1}). With a removal of substituted carbonate, the mineral acquires hydroxyl-ions to maintain charge equilibrium.

Jokei's Cremated Bones

The results of the cremated bone analysis are presented in Table 1. The bone samples contained 1.0–7.5 wt% of bone carbon, whereas nitrogen was not detectable. The carbon contents of the white bone fragments were lower (1.0–1.5 wt%) than those of the black samples (2.9–7.5 wt%). XRD patterns of the cremated bone samples are illustrated in Figure 2a. White bone fragments display sharp peaks at 2θ ~32°, 32.4°, and 33°, whereas black samples display a broad peak. CI values for black, gray, and white samples were 0.21–0.25, 0.30–0.46, and 0.89–1.05, respectively. FTIR spectra of the cremated bone samples are illustrated in Figure 2b. Most IR spectra of the white samples display very little evidence of organic material, with these spectra being similar to those of modern bone heated to 750°C and 900°C. IR spectra of black bone fragments display limited evidence of organic material and carbonate, similar to those of modern bone heated to 600°C. IRSF values for black, gray, and white bone samples were 4.0–4.9, 4.8, and 5.3–7.1, respectively. In a CI vs. IRSF plot (Figure 3a), black and gray samples plot between values for modern bone heated at 450°C and 600°C, whereas white samples plot near 750°C and 900°C values for modern bone. These observations indicate that the black and gray bone fragments were exposed to lower temperature than the white fragments.

The ^{14}C dates of bone apatite in Jokei's cremated bones ranged from 774 BP to 890 BP (Figure 3b), with those for black and gray samples being slightly younger than those of white samples. Furthermore, ^{14}C dates of black samples varied between layers, with upper layer samples displaying younger ages. The ^{14}C dates of the three white samples analyzed were consistent regardless of excavation layer, and the calibrated dates combined using the

https://doi.org/10.1017/RDC.2019.97 Published online by Cambridge University Press

Table 1 Carbon content, $\delta^{13}C$ values, and ^{14}C ages of Jokei's cremated bone samples.

Sample name	Color	XRD CI	IRSF	C_{TOT} (wt%)	C yield[1] (wt%)		$\delta^{13}C$ (‰VPDB)[4]		^{14}C age (BP)(±1σ)				Calibrated date (cal AD)(±2σ)
					Calcite[2]	BA[3]	Calcite	BA[3]	Calcite	(NUTA2-)	Bone	(NUTA2-)	
Jsi-2-B2B	Black	0.25	4.2	3.2	0.35	0.74	–9.1	–16.4	312 ± 29	23656	810 ± 29	23652	1170–1269 (95.4%)
Jsi-2-B2W	White	0.89	5.3	1.5	0.20	0.67	–14.5	–17.2	–394 ± 28	23661	877 ± 30	23654	1042–1105 (24.5%), 1117–1224 (70.9%)
Jsi-2-B3G	Gray	0.30	4.8	2.6	0.40	0.72	–9.3	–16.9	–5 ± 21	22792	774 ± 21	22796	1222–1276 (95.4%)
Jsi-3-B1B	Black	0.21	4.0	7.5	0.45	0.73	–8.5	–15.2	–32 ± 21	22793	818 ± 24	22799	1170–1264 (95.4%)
Jsi-3-B3G	Gray	0.46	4.8	2.5	0.34	0.65	–9.1	–16.7	–59 ± 23	22794	804 ± 21	22800	1194–1196 (0.5%), 1206–1270 (94.9%)
Jsi-4-B3W	White	1.05	7.1	1.1	0.29	0.64	–16.4	–17.1	—	—	875 ± 30	23651	1042–1104 (22.6%), 1117–1224 (72.2%), 1236–1241 (0.6%)
Jsi-4-B4B	Black	0.25	4.9	2.9	0.32	0.71	–8.6	–16.0	495 ± 29	23657	865 ± 30	23653	1046–1090 (13.5%), 1121–1139 (3.5%), 114–1254 (78.4%)
Jsi-4-B4W	White	0.89	5.5	1.0	0.14	0.54	–14.1	–17.5	–158 ± 29	23662	890 ± 30	23655	1040–1108 (35.9%), 1116–1218 (59.5%)

[1]C yield was obtained by dividing the weight of carbon by the weight of bone used for each experiment.
[2]CO_2 released by acetic acid treatment (mainly CO_2 from secondary calcite).
[3]CO_2 from bone apatite.
[4]Errors are ±0.1‰.

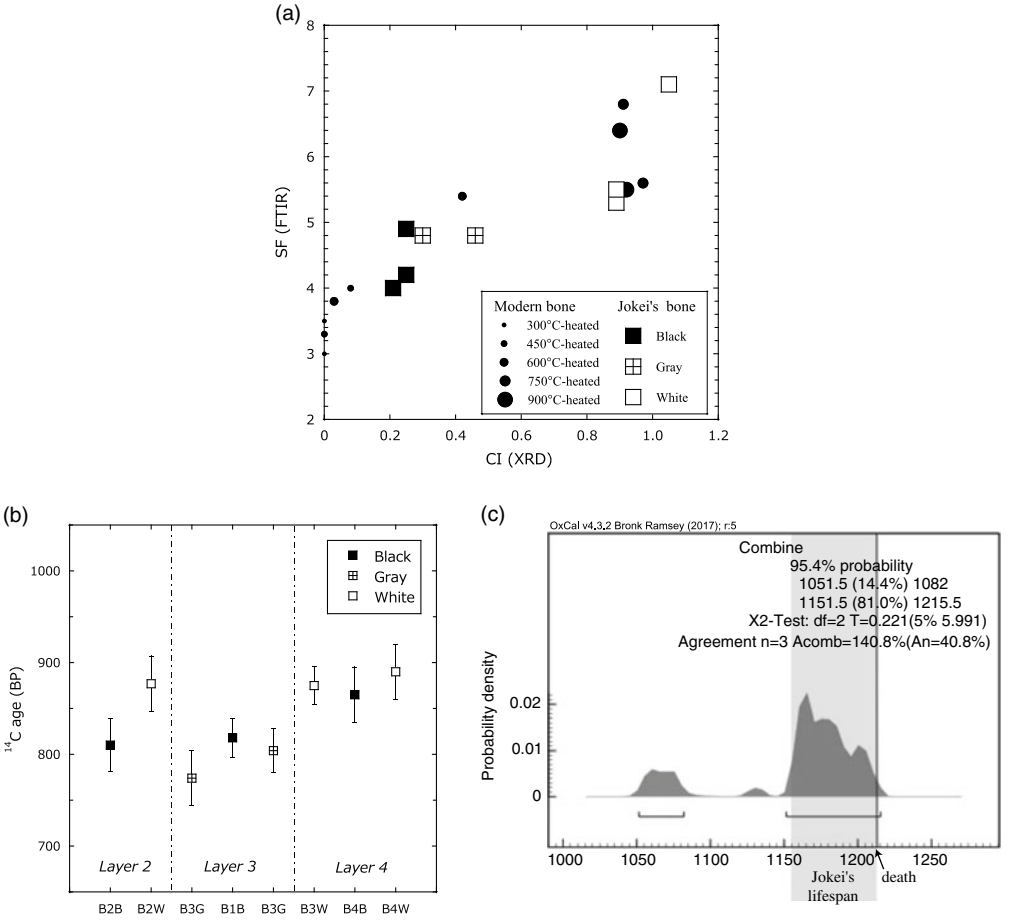

Figure 3 (a) Relationship between CI (XRD) and IRSF (FTIR) for modern bone samples heated at various temperatures (closed circles) and Jokei's cremated bone fragments (black, gray, and white). (b) ^{14}C dates of Jokei's cremated bone samples (±1σ). (c) Combined ^{14}C dates of three white bone fragments.

R_Combine function of the OxCal v.4.3.2 program (Reimer et al. 2013), yielded dates of 1052–1082 cal AD and 1152–1216 cal AD. The latter combined date is consistent with Jokei's lifespan of AD 1155–1213 (Figure 3c). The CO_2 released by the acetic acid treatment gave much younger ^{14}C ages than the CO_2 from bone apatite. The $\delta^{13}C$ values of CO_2 released by the acetic acid treatment of all samples were higher than the $\delta^{13}C$ values of bone apatite, with values of −9.3‰ to −8.5‰ being measured for black and gray bones, and values of −16.4‰ to −14.1‰ being derived for white bones (Table 2).

The concentrations of select alkaline and alkaline earth elements, and phosphorus, from bone and soil samples are presented together with $^{87}Sr/^{86}Sr$ values in Table 2. The concentration ratios of Jsi-2-B2B normalized to Jsi-2-B-B2W, and those of Jsi-4-B4B normalized to Jsi-4-B4W, respectively, are shown in parentheses. Most element concentrations of black bones were similar or a slightly lower than those of white bones, while Ba concentration was significantly higher. This indicates that Ba substituted for Ca in black bones, despite the ionic radius (1.35 Å) of Ba^{2+} being larger than that of Ca^{2+} (1.00 Å). The Ba increase

https://doi.org/10.1017/RDC.2019.97 Published online by Cambridge University Press

Table 2 Chemical and Sr isotope compositions of Jokei's cremated bone samples, modern bone, and soils.

		Jokei's cremated bone						Modern bone	Soil				
		Jsi-2-B2B		Jsi-2-B2W	Jsi-3-B3G	Jsi-4-B4B		Jsi-4-B4W	Go-ino	Jsi-In (bulk)	Jsi-In (ex)	Jsi-S (bulk)	Jsi-S (ex)
Li	ppm	13.2	(1.19)	11.1	10.7	12.4	(0.94)	13.2	0.36	25.8	0.010	19.0	0.041
Be	ppm	0.31	(0.77)	0.41	0.60	0.34	(0.95)	0.36	—	1.5	0.027	1.4	0.046
Na	wt%	0.32	(0.50)	0.64	0.37	0.28	(0.61)	0.47	0.41	0.39	0.0019	1.26	0.0029
Mg	wt%	0.077	(3.98)	0.019	0.051	0.048	(0.79)	0.061	0.35	0.31	0.0030	0.32	0.011
P	wt%	16.9	(1.17)	14.5	14.9	15.2	(1.02)	14.9	16.8	0.20	0.00047	0.04	0.00047
K	wt%	0.0023	(0.32)	0.0072	0.0065	0.0037	(0.50)	0.0073	0.0037	2.25	0.018	2.21	0.024
Ca	wt%	42.7	(1.03)	41.2	41.5	41.2	(0.99)	41.6	41.5	1.23	0.34	0.60	0.042
Rb	ppm	0.063	(0.27)	0.24	0.23	0.14	(0.73)	0.19	0.054	109	2.0	105	0.91
Sr	ppm	500	(0.75)	666	517	459	(0.68)	673	446	87	7.1	114	4.3
Cs	ppm	0.012	(0.65)	0.018	0.022	0.017	(1.70)	0.010	0.005	4.7	0.10	3.4	0.026
Ba	ppm	128	(5.72)	22	81	107	(6.55)	16	77	598	24	600	34
$^{87}Sr/^{86}Sr$		0.709550		0.709233	0.709417	0.709594		0.709227	0.708290	0.711862	0.709841	0.712190	0.709494
Error (2σ)		0.000002		0.000002	0.000002	0.000002		0.000002	0.000002	0.000003	0.000003	0.000002	0.000002

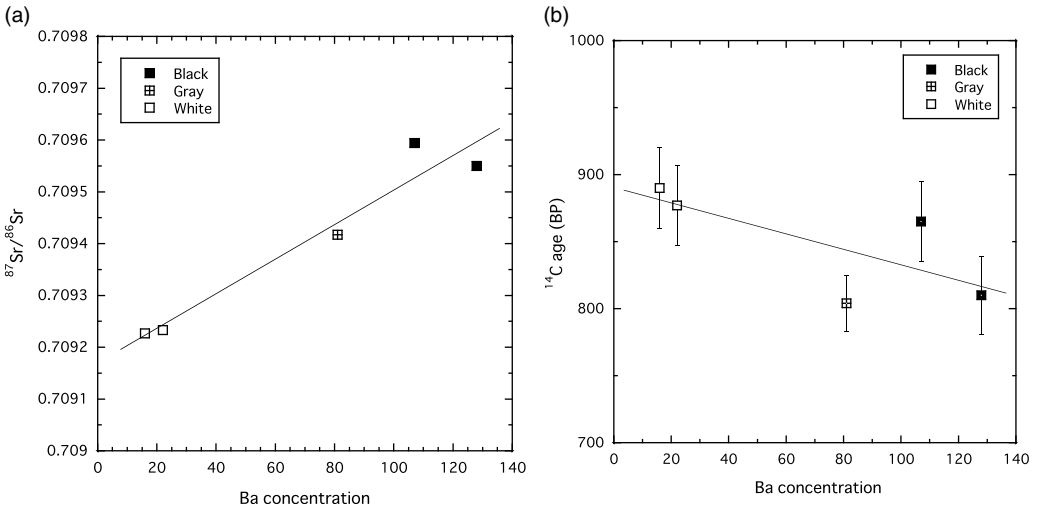

Figure 4 (a) Relationship between Ba concentration and $^{87}Sr/^{86}Sr$. (b) Relationship between Ba concentration and ^{14}C ages for Jokei's cremated bone fragments (black, gray, and white).

is probably related to soil contamination, because Ba concentration in soil is ten times or higher than that found in bone (Table 2). The concentration difference in bone apatite and soil might bring exchange with Ca^{2+} in black bones. Sr concentration in bone apatite may promote higher than that in soil, and therefore decrease in Sr probably occurred by Sr leaching to soil. Mg (Mg^{2+} ionic radius of 0.75 Å) can substitute for Ca, and while Mg concentration increased in sample Jsi-2-B2B, a black bone from Layer 2, Mg concentration in sample Jsi-4-B4B, a black bone from Layer 4, did not increase. The upper layer sample Jsi-2-B2B is likely to have been subjected to a higher degree of contamination by soil than the lower layer sample Jsi-4-B4B, because little soil was found in Layer 4 of the urn. The results suggest that Ba in bone apatite could be more effective for an index of contamination by soil. Figure 4 shows the relationship between Ba concentration and $^{87}Sr/^{86}Sr$ or ^{14}C ages of Jokei's cremated bones. The $^{87}Sr/^{86}Sr$ values become higher with increase of Ba concentration and get closer to the $^{87}Sr/^{86}Sr$ of soil, especially the exchangeable Sr fraction of soil (Figure 4a). The ^{14}C ages become younger with increase in Ba concentration, though the trend is not as clear as in the $^{87}Sr/^{86}Sr$ values.

DISCUSSION

Structural Changes in Bone During Heating

The XRD patterns of the modern bones indicate that bone apatite has low crystallinity in unheated bone due to the presence of organic polymers; these strongly interfere with diffraction of crystalline apatite (Pramanik et al. 2013). As temperature increases, the collagen polymer molecules disintegrate, with almost all fibrils having been burnt out by 500°C, and by 600°C virtually all organic matter is destroyed. The crystallinity of bone apatite increases with increasing temperature, particularly between 600°C and 750°C. The 600–750°C gap is indicated in the CI vs. IRSF diagram (Figure 3a). Wopenka and Pasteris (2005) reported an absence of OH^- in bone apatite based on the results obtained via Raman spectroscopy. The lack of OH^- ions in bone apatite may be attributable to the

https://doi.org/10.1017/RDC.2019.97 Published online by Cambridge University Press

presence of CO_3^{2-}. The substituted carbonate is likely to limit crystal size, and a high concentration of carbonate in bone apatite plays an important role in constraining bone crystallites on the nanometer scale. As carbonate is removed during the burning, hydroxyl ions are added to bone apatite, leading to an increase in crystallinity at > 600°C. Above this temperature, carbon content is considered to correspond with crystallinity of apatite. In this study, the carbon contents of bone apatite in the white bone fragments were measured to be lower (0.54–0.67 wt%) than those in the gray samples (0.65 and 0.72 wt%) and the black samples (0.71–0.73 wt%). However, the difference between these values is small, and the ranges overlap. These observations suggest that % carbon in bone apatite is helpful for screening samples as a first step but may not provide sufficient resolution to be used as an index for evaluating the reliability of ^{14}C dates.

Radiocarbon Dating of Archeological Cremated Bones

The ^{14}C ages of the white Jokei bone fragments were consistent with his lifespan (Figure 3c). The IR spectra and XRD patterns of those samples are similar to those of modern bone heated to 750°C and 900°C, assuming that they were heated at higher temperatures. It should be noted, however, cremation experiments are not representative of real cremations, and post-burial duration also influences the degree of mineralogical changes. High-temperature (> 750°C) cremated bones with high apatite crystallinity are often resistant to diagenetic alteration and such bone apatite tends to record limited isotopic exchange (Lanting et al. 2001). The white Jokei bone fragments seem to have experienced high temperatures during cremation, showing high crystallinity and show low Ba concentration, which indicates limited isotope exchange during deposition, and renders measured ^{14}C age and $^{87}Sr/^{86}Sr$ reliable. Meanwhile, the black Jokei bone fragments tend to show younger ^{14}C ages and higher $^{87}Sr/^{86}Sr$ than the white bone fragments. The black bones display IR spectra and XRD patterns similar to modern bones heated at 450°C and 600°C, indicating that they were heated at temperatures lower than 750°C, and have low apatite crystallinity and high Ba concentration. Therefore, bone apatite in the black bone fragments may have undergone limited isotopic exchange into bone apatite. The higher carbon yield in the black bone samples suggests the existence of exogenous carbon in the bone apatite, though there is little carbon increase. In a single case, sample Jsi-4-B4B, a black bone from Layer 4, gave a similar ^{14}C age to the white bones, possibly due to less soil contamination.

All ^{14}C ages of CO_2 released by the acetic acid treatment (mainly secondary calcite) were much younger than ^{14}C ages derived directly from bone apatite. This suggests that contaminant, consisting mostly of secondary calcites with a younger age, was removed effectively by pretreatment using 0.1 M acetic acid for 1 hr. However, the pretreatment may be not sufficient to completely remove contaminant from black bones heated at lower temperatures. The older ^{14}C ages of CO_2 released from black bones by acetic acid treatment, compared with ages from the white bones, showed that innate carbon in bone apatite may be removed along with secondary calcite. In black bones heated at temperatures lower than 750°C, which have low apatite crystallinity, contaminant carbon may have been exchanged with carbon from within the apatite crystal structure. This indicates the isotopic exchange of carbon between bone apatite and adsorbed CO_2, and exogenous carbon, either environmentally formed or modified during burning, in the black samples. Therefore, for reliable ^{14}C dating in cremated bone samples, it is necessary to check the crystallinity of bone apatite and perform chemical indexing to identify processes such as Ba capture, in order to confirm the quality of measured ^{14}C dates.

https://doi.org/10.1017/RDC.2019.97 Published online by Cambridge University Press

CONCLUSIONS

Cremated human bone fragments of different colors, excavated in Japan, were analyzed and dated. White fragments displayed the highest CI and IRSF values, similar to those of modern bone heated at 750–900°C, and low Ba concentration. The measured ^{14}C age was consistent with the historical year of death. Black bone fragments displayed low crystallinity, higher Ba concentration, higher $^{87}Sr/^{86}Sr$ values close to the soil value, and a younger ^{14}C age. These results indicate that bone apatite in white cremated bone is resistant to diagenetic alteration and can provide reliable ^{14}C dates, while bone apatite in black and gray bones is affected by soil contamination and is unlikely to provide reliable ^{14}C dates. The results of this study indicate that it is important to check the crystallinity of apatite, and to estimate the influence of soil contamination in cremated bone samples using chemical indexes such as Ba capture, to ensure reliable ^{14}C dating.

ACKNOWLEDGMENTS

We thank H. Kagi of the University of Tokyo for FTIR analysis, K. Mimura of Nagoya University for elemental analysis, and T. Kato of Nagoya University for XRD analysis. We also thank A. Sato of the Gangoji Institute for Research of Cultural Property for providing us with Jokei's cremated bone samples, and K. Suzuki of Nagoya University for the modern wild boar bones. This study was supported by the Japan Society for the Promotion of Science, Grant-in-Aid for Challenging Exploratory Research (No. 26560144).

REFERENCES

Balter V, Saliège J-F, Bocherens H, Person A. 2002. Evidence of physico-chemical and isotopic modifications in archaeological bones during controlled acid etching. Archaeometry 44: 329–336.

Berger R, Horney AG, Libby WF. 1964. Radiocarbon dating of bone and shell from their organic components. Science 144(3621):999–1001.

Bronk Ramsey C. 2009. Bayesian analysis of radiocarbon dates. Radiocarbon 51(1):337–360.

Cazalbou S, Combes C, Eichert D, Rey C. 2004. Adaptive physico-chemistry of bio-related calcium phosphates. Journal of Materials Chemistry 14:2148–2153.

Ericson JE. 1985. Strontium isotope characterization in the study of prehistoric human ecology. Journal of Human Evolution 14:503–514.

Hodell DA, Quinn RL, Brenner M, Kamenov G. 2004. Spatial variation of strontium isotopes ($^{87}Sr/^{86}Sr$) in the Maya region: a tool for tracking ancient human migration. Journal of Archaeological Science 31:585–601.

Hüls CM, Erlenkeuser H, Nadeau MJ, Grootes PM, Andersen N. 2010. Experimental study on the origin of cremated bone apatite carbon. Radiocarbon 52(2–3):587–599.

Lanting JN, Aerts-Bijma AT, van der Plicht J. 2001. Dating of cremated bones. Radiocarbon 43(2A): 249–254.

Minami M, Kato T, Miyata Y, Nakamura T, Hua Q. 2013. Small-mass AMS radiocarbon analysis at Nagoya University. Nuclear Instruments and Methods in Physics Research B 294: 91–96.

Minami M, Suzuki K. 2018. $^{87}Sr/^{86}Sr$ compositional linkage between geological and biological materials: A case study from the Toyota granite region of Japan. Chemical Geology 484:224–232.

Mukumoto H, Minami M, Nakamura T. 2017. Research report on Gorinto tower dedicated to Gedatsu Shonin Jokei, and urn excavated under the tower in the Jisho-in Temple, Sango-cho, Nara Prefecture 10. Gangoji Institute for Research of Cultural Property.

Munro LE, Longstaffe FJ, White CD. 2008. Effects of heating on the carbon and oxygen-isotope compositions of structural carbonate in bioapatite from modern deer bone. Palaeogeography, Palaeoclimatology, Palaeoecology 266:142–150.

Olson EA, Broecker WS. 1961. Lamont Natural Radiocarbon Measurements VII. Radiocarbon 3:141–175.

Olsen J, Heinemeier J, Bennike P, Krause C, Hornstrup KM, Thrane H. 2008. Characterisation and blind testing of radiocarbon dating of cremated bone. Journal of Archaeological Science 35(3):791–800.

Person A, Bocherens H, Saliège J-F, Paris F, Zeitoun V, Gérard M. 1995. Early diagenetic evolution of bone phosphate: an X-ray diffractometry

https://doi.org/10.1017/RDC.2019.97 Published online by Cambridge University Press

analysis. Journal of Archaeological Science 22(2):211–221.

Prince TD, Burton JH, Bentley RA. 2002. The characterization of biologically available strontium isotope ratios for the study of prehistoric migration. Archaeometry 44:117–135.

Pramanik S, Hanif ASM, Pingguan-Murphy B, Abu Osman, NA. 2013. Morphological changes of heat treated bovine bone: a comparative study. Materials 6:65–75.

Reimer PJ, Bard E, Bayliss A, Beck JW, Blackwell PG, Bronk Ramsey C, Buck CE, Cheng H, Edwards RL, Friedrich M, Grootes PM, Guilderson TP, Hajdas I, Hatté C, Heaton TJ, Hoffmann DI, Hogg AG, Hughen KA, Kaiser KF, Kromer B, Manning SW, Niu M, Reimer RW, Richards DA, Scott EM, Southon JR, Staff RA, Turney CSM, van der Plicht J. 2013. IntCal13 and Marine13 radiocarbon age calibration curves, 0–50,000 years cal BP. Radiocarbon 55(4):1869–1887.

Snoeck C, Brock F, Schulting RJ. 2014. Carbon exchanges between bone apatite and fuels during cremation: Impact on radiocarbon dates. Radiocarbon 56(2):591–602.

Surovell TA. 2000. Radiocarbon dating of bone apatite by step heating. Geoarchaeology 15(6):591–608.

Thornton EK 2011. Reconstructing ancient Maya animal trade through strontium isotope ($^{87}Sr/^{86}Sr$) analysis. Journal of Archaeological Science 38:3254–3263.

Weiner S, Bar-Yosef O. 1990. States of preservation of bones from prehistoric sites in the Near East: a survey. Journal of Archaeological Science 17(2):187–196.

Wopenka B, Pasteris JD. 2005. A mineralogical perspective on the apatite in bone. Materials Science and Engineering C 25(2):131–143.

Zazzo A, Saliège J-F, Person A, Boucher H. 2009. Radiocarbon dating of calcined bones: Where does the carbon come from? Radiocarbon 51(2):1–12.

Zazzo A, Lebon M, Chiotti L, Comby C, Delqué-Količ E, Nespoulet R, Reiche I. 2013. Can we use calcined bones for ^{14}C dating the Paleolithic? Radiocarbon 55(2–3):1409–1421.

https://doi.org/10.1017/RDC.2019.97 Published online by Cambridge University Press